Atmos. Chem. Phys., 13, 8457–8470, 2013
www.atmos-chem-phys.net/13/8457/2013/
doi:10.5194/acp-13-8457-2013

Atmospheric Chemistry and Physics Open Access

Investigating the influences of SO_2 and NH_3 levels on isoprene-derived secondary organic aerosol formation using conditional sampling approaches

Y.-H. Lin[1], E. M. Knipping[2], E. S. Edgerton[3], S. L. Shaw[4], and J. D. Surratt[1]

[1]Department of Environmental Sciences and Engineering, Gillings School of Global Public Health, The University of North Carolina at Chapel Hill, Chapel Hill, NC, USA
[2]Electric Power Research Institute, Washington, D.C., USA
[3]Atmospheric Research & Analysis, Inc., Cary, NC, USA
[4]Electric Power Research Institute, Palo Alto, CA, USA

Correspondence to: J. D. Surratt (surratt@unc.edu)

Received: 31 December 2012 – Published in Atmos. Chem. Phys. Discuss.: 1 February 2013
Revised: 24 June 2013 – Accepted: 13 July 2013 – Published: 27 August 2013

Abstract. Filter-based $PM_{2.5}$ samples were chemically analyzed to investigate secondary organic aerosol (SOA) formation from isoprene in a rural atmosphere of the southeastern US influenced by both anthropogenic sulfur dioxide (SO_2) and ammonia (NH_3) emissions. Daytime $PM_{2.5}$ samples were collected during summer 2010 using conditional sampling approaches based on pre-defined high and low SO_2 or NH_3 thresholds. Known molecular-level tracers for isoprene SOA formation, including 2-methylglyceric acid, 3-methyltetrahydrofuran-3,4-diols, 2-methyltetrols, C_5-alkene triols, dimers, and organosulfate derivatives, were identified and quantified by gas chromatography coupled to electron ionization mass spectrometry (GC/EI-MS) and ultra performance liquid chromatography coupled to electrospray ionization high-resolution quadrupole time-of-flight mass spectrometry (UPLC/ESI-HR-Q-TOFMS). Mass concentrations of six isoprene low-NO_x SOA tracers contributed to 12–19 % of total organic matter (OM) in $PM_{2.5}$ samples collected during the sampling period, indicating the importance of the hydroxyl radical (OH)-initiated oxidation (so-called photooxidation) of isoprene under low-NO_x conditions that lead to SOA formation through reactive uptake of gaseous isoprene epoxydiols (IEPOX) in this region. The contribution of the IEPOX-derived SOA tracers to total organic matter was enhanced by 1.4 % ($p = 0.012$) under high-SO_2 sampling scenarios, although only weak associations between aerosol acidity and mass of IEPOX SOA tracers were observed. This suggests that IEPOX-derived SOA formation might be modulated by other factors simultaneously, rather than only aerosol acidity. No clear associations between isoprene SOA formation and high or low NH_3 conditional samples were found. Positive correlations between sulfate aerosol loadings and IEPOX-derived SOA tracers for samples collected under all conditions indicates that sulfate aerosol could be a surrogate for surface accommodation in the uptake of IEPOX onto preexisting aerosols.

1 Introduction

Tropospheric fine aerosols ($PM_{2.5}$, with aerodynamic diameter $\leq 2.5\,\mu m$) have been recognized to have significant influences on regional air quality, climate change, and human health (Kanakidou et al., 2005; Hallquist et al., 2009). Organic aerosol constituents that usually account for a large fraction (i.e., 20–90 %) of the total $PM_{2.5}$ mass are of particular concern, especially due to their high degree of chemical complexity that results in limited understanding of their sources, sinks, and chemical structure, thus yielding major uncertainties for air quality modeling and human health risk assessment.

Secondary organic aerosol (SOA) that originates from the photochemical oxidation of biogenic volatile organic compounds (BVOCs) is thought to be the largest contributor

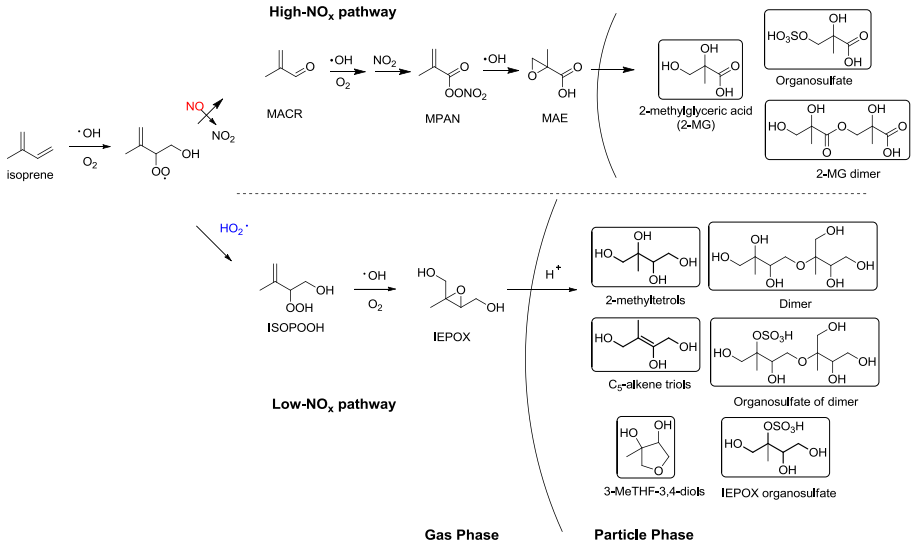

Fig. 1. Proposed chemistry leading to isoprene SOA: NO_x-dependent pathways (Surratt et al., 2010; Lin et al., 2013). For simplicity, only the cis-β-IEPOX isomer is shown for IEPOX in the low-NO_x (or NO-limited) pathway.

to the global SOA burden, owing to large emissions and efficient SOA formation processes (Chung and Seinfeld, 2002; Kanakidou et al., 2005; Henze and Seinfeld, 2006). The atmospheric significance of biogenic secondary organic aerosol (BSOA) has been inferred from recent remote sensing data over the southeastern United States, which suggests BVOC emissions combine with anthropogenic pollutants (e.g., SO_2, NO_x, and primary OC emissions), leading to substantial amounts of SOA observed in this region (Goldstein et al., 2009). The enhancement of SOA from BVOCs in this region highlights the need for further research aimed at understanding the attributable sources and detailed mechanisms leading to BSOA formation in order to develop effective control strategies.

Recently, organosulfate formation was reported through reactive uptake of BVOC oxidation products onto acidified sulfate seed aerosols, providing a likely link between anthropogenic pollutants and the enhanced BSOA formation (Iinuma et al., 2007, 2009; Surratt et al., 2007a, 2008). Moreover, the effects of acid-catalyzed enhancement on BSOA formation have also been observed in several laboratory studies (Iinuma et al., 2004; Surratt et al., 2007b; Offenberg et al., 2009; Chan et al., 2011). In the presence of anthropogenic pollutants, such as nitric acid and sulfuric acid produced from the oxidation of NO_x and SO_2, SOA mass yields from isoprene under high- and low-NO_x conditions, respectively, have been shown to increase substantially (i.e., from 1–3 % to 3–30 %) with preexisting acidified sulfate aerosols in the laboratory (Chan et al., 2010a; Surratt et al., 2010). Figure 1 displays the NO_x-dependent isoprene SOA formation mechanisms. Under high-NO_x conditions, isoprene SOA is enhanced with increasing NO_2/NO ratios (Chan et al., 2010a; Surratt et al., 2010). This enhancement is explained by the formation and subsequent photooxidation of methacryloylperoxynitrate (MPAN) (Surratt et al., 2010), forming methacrylic acid epoxide (MAE) (Lin et al., 2013), which leads to 2-methylglyceric acid (2-MG) formation and its corresponding oligoesters (Surratt et al., 2006, 2010). Notably, 2-MG has been used as one of the isoprene SOA tracer compounds in the organic tracer-based source apportionment method developed by Kleindienst et al. (2007) to estimate the contributions of BVOCs to SOA formation. On the other hand, under low-NO_x (i.e., NO-limited) conditions, isoprene SOA has been observed to be enhanced in the presence of acidified sulfate seed aerosols (mass yield $\sim$ 29 %) over that in the presence of neutral seed aerosols (mass yield $\sim$ 1 %) (Surratt et al., 2010). Increased uptake of gaseous isoprene epoxydiols (IEPOX) by enhanced particle-phase acid-catalyzed oxirane ring-opening reaction rates has been proposed and demonstrated to explain this enhancement (Minerath et al., 2009; Eddingsaas et al., 2010; Surratt et al., 2010; Lin et al., 2012). Identification of known isoprene low-NO_x SOA tracers through reactive uptake of IEPOX onto acidified sulfate seed aerosols also supports this hypothesis (Surratt et al., 2010; Lin et al., 2012). Although clear evidence of acid-catalyzed enhancement for BSOA formation has been shown in laboratory studies, the importance of aerosol acidity on ambient BSOA formation remains unclear, owing to the fact that acidified sulfate seed aerosols used in the laboratory studies were usually much more acidic than the acidity measured in ambient aerosols (Edgerton et al., 2007; Tanner et al., 2009). In addition, ambient aerosol acidity is also likely modulated by other environmental factors, such as the atmospheric alkaline species (e.g., NH_3) that leads to the neutralization of acidic aerosols (Huntzicker et al., 1980; McMurry et al., 1983), but the uptake processes

and the kinetics in the atmosphere have yet to be fully elucidated (Huang et al., 2011; Yao et al., 2011; Liggio et al., 2011).

In the present study, $PM_{2.5}$ samples were collected to investigate the effects of ambient aerosol acidity on BSOA formation in a rural atmosphere under the influences of anthropogenic SO_2 and NH_3 emissions. Filter samples were collected from Yorkville, GA, a rural site located within the Southeastern Aerosol Research and Characterization Study (SEARCH) network during the summer of 2010. This site is characterized by high isoprene emissions during summertime, and is influenced by SO_2 point sources from local coal-fired power plants (Edgerton et al., 2006a) as well as NH_3 emissions from nearby poultry operations (Edgerton et al., 2007). Conditional sampling strategies were employed in this study to collect $PM_{2.5}$ samples under predefined environmental thresholds (i.e., the mixing ratios of SO_2 or NH_3) to distinguish the influences of ambient SO_2 and NH_3 levels on ambient aerosol acidity and BSOA formation. More specifically, known isoprene SOA tracers (which include organosulfate derivatives) were chemically characterized by UPLC/ESI-HR-Q-TOFMS (ultra performance liquid chromatography coupled to electrospray ionization high-resolution quadrupole time-of-flight mass spectrometry) and GC/EI-MS (gas chromatography coupled to electron ionization mass spectrometry) techniques to measure SOA constituents at the molecular level. The effects of acid enhancement on BSOA formation were examined by comparing paired samples collected under high and low SO_2 or NH_3 scenarios. Even though some of these BSOA tracers have been previously characterized from $PM_{2.5}$ samples collected from the SEARCH network in a time-integrated manner (Chan et al., 2010b; Gao et al., 2006; Surratt et al., 2007a, 2008), using conditional sampling approaches to collect $PM_{2.5}$ in this study is to our knowledge one of the first attempts to systematically examine if BSOA formation is enhanced or suppressed due to anthropogenic emissions in this region.

2 Experimental section

2.1 Collection of $PM_{2.5}$ by conditional sampling

$PM_{2.5}$ samples were collected from Yorkville (YRK), GA, a rural site located $\sim$55 km west northwest of Atlanta, GA, within the SEARCH network during summer 2010. The detailed site descriptions are provided in the SEARCH overview papers (Hansen et al., 2003; Edgerton et al., 2005, 2006b). In the present work, paired quartz filter samples were collected by conditional sampling approaches based on the measured SO_2 or NH_3 mixing ratios. Concentration thresholds were set to (1) distinguish the influences of SO_2 or NH_3 levels on ambient aerosol acidity and isoprene SOA formation; (2) ensure that sufficient material was collected for chemical analysis; and (3) avoid motor burnout by activating the samplers too frequently. The pre-defined high and low SO_2 or NH_3 thresholds were determined by the review of historical ambient data at the sampling site. For SO_2, data from June to August 2009 were analyzed and the thresholds were set to correspond to the lowest 40 % and highest 40 % of observed 1 min concentrations. We focused on 2009 because installation of emission controls on nearby power plants caused concentrations subsequent to 2008 to be significantly lower than 2008 and before. For NH_3, we analyzed the same months of data for three consecutive years (2007–2009) and set thresholds to correspond approximately to the lowest 20 % and highest 40 % of observed 1 min values.

2.1.1 SO_2 conditional sampling

SO_2 conditional samples were collected from 25 June 2010 until 14 July 2010 between 09:00 and 18:59 local standard time. Two Tisch Environmental (Cleves, OH) Model TE-6070V-2.5 high-volume $PM_{2.5}$ air samplers were operated side-by-side to collect aerosol samples at a flow rate of 1 $m^3\,min^{-1}$ during the day (09:00–18:59 LT). One high-volume $PM_{2.5}$ sampler was designated as the high-SO_2 sampler, which was only turned on to collect $PM_{2.5}$ samples when the measured SO_2 mixing ratios were ≥ 0.5 ppbv. The second high-volume $PM_{2.5}$ sampler was only turned on to collect aerosol samples when the SO_2 mixing ratios were ≤ 0.25 ppbv, and this sampler was designated as the low-SO_2 sampler. SO_2 was measured with 1 min time resolution using a Thermo-Environmental (Franklin, MA) Model 43c pulsed fluorescence SO_2 analyzer.

2.1.2 NH_3 conditional sampling

NH_3 conditional samples were collected from 29 July 2010 until 6 August 2010. The same conditional sampling approaches described above were employed to collect $PM_{2.5}$ samples based on the NH_3 mixing ratios during the day (09:00–18:59 LT). The high-NH_3 sampler only collected $PM_{2.5}$ samples when the NH_3 mixing ratios were ≥ 2 ppbv, while the low-NH_3 sampler only collected aerosol samples when the NH_3 mixing ratios were ≤ 1 ppbv. NH_3 was measured with 1 min time resolution via continuous denuder difference with a Thermo-Environmental Model 42c chemiluminescence NO-NO_x analyzer. The NO-NO_x analyzer was modified to measure NH_3 as described in Saylor et al. (2010).

Available collocated measurements and meteorological data during the conditional sampling periods are summarized in Table 1.

2.2 Filter extractions and chemical analyses for isoprene SOA tracers

Known isoprene SOA tracers, including 2-methyltetrols (Claeys et al., 2004), C_5-alkene triols (Wang et al.,

Table 1. Summary of average meteorological data and complementary collocated measurements.

Condition	High SO_2	Low SO_2	High NH_3	Low NH_3
Sampling Period	25 Jun 2010–14 Jul 2010		29 Jul 2010–6 Aug 2010	
O_3 (ppb)	46.9 ± 3.0	46.1 ± 2.6	43.4 ± 3.5	48.7 ± 3.5
CO (ppb)	141.8 ± 4.6	145.7 ± 6.6	167.7 ± 10.2	161.1 ± 11.3
SO_2 (ppb)	1.1 ± 0.1	0.2 ± 0.0	0.7 ± 0.3	0.7 ± 0.2
NO (ppb)	0.2 ± 0.0	0.2 ± 0.0	0.3 ± 0.1	0.2 ± 0.0
NO_2 (ppb)	1.2 ± 0.2	1.1 ± 0.2	1.3 ± 0.4	1.5 ± 0.4
NO_y (ppb)	2.8 ± 0.3	2.6 ± 0.3	3.0 ± 0.5	2.9 ± 0.4
HNO_3 (ppb)	0.6 ± 0.0	0.6 ± 0.1	0.6 ± 0.1	0.6 ± 0.1
NH_3 (ppb)	2.2 ± 0.4	2.3 ± 0.4	2.6 ± 0.3	1.4 ± 0.2
NEPH (Mm^{-1})	50.1 ± 3.4	47.6 ± 4.6	71.8 ± 7.4	65.1 ± 9.6
SO_4^{2-} ($\mu g\,m^{-3}$)	4.1 ± 0.4	3.5 ± 0.5	3.3 ± 0.3	3.3 ± 0.3
NO_3^- ($\mu g\,m^{-3}$)	0.2 ± 0.0	0.2 ± 0.1	0.3 ± 0.1	0.2 ± 0.1
NH_4^+ ($\mu g\,m^{-3}$)	1.4 ± 0.1	1.3 ± 0.1	1.6 ± 0.2	1.4 ± 0.2
BC ($\mu g\,m^{-3}$)	0.3 ± 0.0	0.3 ± 0.0	0.3 ± 0.0	0.3 ± 0.1
OC ($\mu g\,m^{-3}$)	3.2 ± 0.1	3.1 ± 0.3	3.6 ± 0.2	3.3 ± 0.3
$PM_{2.5}$ ($\mu g\,m^{-3}$)	13.5 ± 0.8	12.2 ± 1.1	16.1 ± 1.2	14.9 ± 2.0
Temp (°C)	27.4 ± 0.4	27.4 ± 0.7	29.3 ± 1.0	29.2 ± 0.6
RH (%)	66.3 ± 2.5	65.7 ± 3.0	67.1 ± 4.8	66.5 ± 3.6
BP (mbar)	969.9 ± 0.7	969.3 ± 0.7	968.4 ± 0.9	967.5 ± 0.7
SR ($W\,m^{-2}$)	526.2 ± 44.1	461.5 ± 42.0	600.8 ± 69.7	290.6 ± 48.5

2005), 3-methyltetrahydrofuran-3,4-diols (3-MeTHF-3,4-diols) (Lin et al., 2012; Zhang et al., 2012), IEPOX-derived dimers (Surratt et al., 2006), and 2-MG (Edney et al., 2005) were characterized by GC/MS with prior trimethylsilylation using electron ionization (EI). A quarter of each 8×10-inch quartz filter sample was extracted in pre-cleaned scintillation vials with 20 mL high-purity methanol (LC-MS CHROMASOLV-grade, Sigma-Aldrich) under 45 min of sonication. The filter extracts were filtered through 0.2 µm PTFE syringe filters (Pall Life Science, Acrodisc®) to remove suspended quartz filter fibers and insoluble particles, and subsequently blown to dryness under a gentle N_2 stream at room temperature. Residues of the filter extracts were immediately trimethylsilylated by reacting with 100 µL of BSTFA + TMCS (99 : 1 v/v, Supelco) and 50 µL of pyridine (anhydrous, 99.8 %, Sigma-Aldrich) at 70 °C for 1 h. The derivatized samples were analyzed by GC/MS within 24 h after trimethylsilylation. GC/MS analysis was performed using a Hewlett-Packard (HP) 5890 Series II Gas Chromatograph coupled to a HP 5971A Mass Selective Detector. An *Econo-Cap®-EC®-5* Capillary Column (30 m × 0.25 mm i.d.; 0.25 µm film thickness) was used to separate the trimethylsilyl (TMS) derivatives before MS detection. 1 µL of each derivatized sample was injected onto the GC column. Operating conditions and the temperature program of the GC/MS procedure were as described previously by Surratt et al. (2010). Isoprene SOA tracers were quantified with the following base peak ion fragments: m/z 219 for 2-methyltetrols, m/z 231 for C_5-alkene triols, m/z 262 for 3-MeTHF-3,4-diols, m/z 335 for dimers, and m/z 219 for 2-MG. *Meso*-erythritol (≥ 99 %, Sigma), a structurally similar analog of 2-methyltetrols, was used as a surrogate standard to quantify 2-methyltetrols, C_5-alkene triols, dimers, and 2-MG in the $PM_{2.5}$ samples. The ion fragment of m/z 217 was used for *meso*-erythritol for quantification. 3-MeTHF-3,4-diols were quantified using synthesized authentic standards. The details of the synthesis procedures are reported in Zhang et al. (2012).

Characterization of organosulfate derivatives was performed using ultra performance liquid chromatography interfaced to a high-resolution quadrupole time-of-flight mass spectrometer (Agilent 6500 Series) equipped with an electrospray ionization source (UPLC/ESI-HR-Q-TOFMS) operated in the negative (–) ion mode. A Waters ACQUITY UPLC HSS T3 column (2.1 × 100 mm, 1.8 µm particle size) was used for chromatographic separations. Detailed UPLC/(–)ESI-HR-Q-TOFMS operating conditions can be found in Zhang et al. (2011). Quartz filter samples for UPLC/(–)ESI-HR-Q-TOFMS analyses were extracted in the same manner as those for GC/MS analyses. After the filter extracts were blown dry, the extract residues were reconstituted with 150 µL of a 50 : 50 (v/v) solvent mixture of methanol containing 0.1 % acetic acid (LC-MS CHROMASOLV-grade, Sigma-Aldrich) and water containing 0.1 % acetic acid (LC-MS CHROMASOLV-grade, Sigma-Aldrich). 5 µL of each sample was injected onto the UPLC column eluted with solvent of the same composition. Isoprene-derived organosulfate species reported previously

by Surratt et al. (2008) were identified and quantified. The elemental composition of target compounds was assigned based on accurate mass data. The errors of accurate mass fittings were within ±1 mDa. Owing to the lack of authentic standards, sodium propyl sulfate (electronic grade, City Chemical LLC) was used to quantify all isoprene-derived organosulfates. The use of sodium propyl sulfate to quantify isoprene-derived organosulfates was performed under the assumption of similar ionization efficiency since the retention time (and thus the mobile phase composition) of this surrogate standard is similar to our target analytes. The quantification was done based on the mass response. The detection limit of sodium propyl sulfate on UPLC/(–)ESI-HR-TOFMS was 0.01 ng μL^{-1}, determined by signal-to-noise ratios of 3 : 1.

The efficiency of the extraction protocols was evaluated by spiking 5 replicates of pre-baked blank quartz filters with quantifying standards. Extraction efficiencies (62–82 %) are taken into account for SOA constituents that were quantified in the field samples.

2.3 Inorganic ion measurements

Continuous sulfate (SO_4^{2-}), nitrate (NO_3^-), and ammonium (NH_4^+) measurements were made during the sampling periods at the site using continuous particle analyzers; detailed instrumental setup and operating conditions of these analyzers have been described elsewhere (Edgerton et al., 2006b). Briefly, continuous SO_4^{2-} measurements were made using a variation of the Harvard School of Public Health approach. A high temperature (> 850 °C) stainless steel tube was used to reduce particle SO_4^{2-} to SO_2. Then SO_2 was measured by a Thermo-Environmental Instruments Model 43s or 43ctl high-sensitivity, pulsed ultraviolet fluorescence SO_2 analyzer. Continuous NO_3^- and NH_4^+ measurements were made using a three-channel continuous differencing approach developed by ARA, Inc. Air samples were drawn through the inlet and series of denuders coated with sodium carbonate and citric acid followed by an activated carbon honeycomb denuder to remove interferents, and then the flow was split into three analytical channels that converted different nitrogen species to NO, depending on temperature. Channel 1 (CH1) measured the baseline gas-phase NO_y for the analyzer by passing the air through a 2 µm Teflon filter, followed by a KCl-coated filter and a molybdenum (Mo) mesh catalyst heated to 350 °C. Channel 2 (CH2) measured the baseline NO_y plus particle-bound NO_3^- by passing air through Mo converter at 350 °C without filtration. Channel 3 (CH3) measured NH_4^+ plus baseline NO_y and particle-bound NO_3^- by flowing air through ceramic tube containing platinum (Pt) catalyst heated to 600 °C, followed by another Mo converter at 350 °C. NO_3^- and NH_4^+ concentrations were calculated as CH2-CH1 and CH3-CH2, respectively. Continuous inorganic data were processed in a time-weighted manner to represent the real-time aerosol inorganic conditions to estimate ambient aerosol acidity.

Filter-based inorganic measurements were also performed by analyzing a 37 mm filter punch from each quartz filter sample. Filter samples were extracted with 15 mL Millipore 18.2 Megohm Ultrapure DI H_2O. A Dionex ICS-3000 Ion Chromatography System was used to quantify SO_4^{2-}, NO_3^-, and NH_4^+ concentrations in filter extracts. The anion channel included a Dionex AG18 guard column, a Dionex AS18 analytical column and 10 mM KOH eluent. The cation channel included a Dionex CG16 guard column, a Dionex CS16 analytical column and 18 mM methanesulfonic acid eluent. The ICS-3000 was calibrated with NIST-traceable multi-element standards covering the range of observed concentrations. Sample injection volumes were 1.0 mL and peak area was used for quantification. Analytical detection limits were in the range of 2–3 µg L^{-1}, and analytical uncertainties were < 5 %. Measured concentrations were compared with continuous inorganic measurements to evaluate the changes of inorganic composition during sample storage.

2.4 Calculation of aerosol acidity

Ambient aerosol acidity of the collected $PM_{2.5}$ samples was estimated by calculating the degree of stoichiometric neutralization, defined as the molar ratios of NH_4^+ to the sum of SO_4^{2-} and NO_3^-, assuming aerosol SO_4^{2-} and NO_3^- were only associated with NH_4^+ and H^+. Acidic aerosols are characterized by having a neutralization degree less than unity. The neutralization degree greater than unity implies the samples are fully neutralized.

$$\text{Neutralization degree} = [NH_4^+]/(2 \times [SO_4^{2-}] + [NO_3^-]) \quad (1)$$

In addition, an on-line version of the extended aerosol thermodynamics model (E-AIM II: H^+-NH_4^+-SO_4^{2-}-NO_3^--H_2O) was used to estimate aerosol acidity by calculating the in situ aerosol pH in the particle aqueous phase (Clegg et al., 1998). Inputs of free [H^+] were calculated based on charge balance from measured NH_4^+, SO_4^{2-}, and NO_3^- concentrations. Temperature and relative humidity (RH) parameters were obtained from the measurements at the sampling site.

$$[H^+]_{\text{free}} = (2 \times [SO_4^{2-}] + [NO_3^-]) - [NH_4^+] \quad (2)$$

Modeling outputs of activity coefficient and moles of H_{aq}^+ in the aqueous phase, and the total volume of aqueous phase in the aerosol per m^3 air in the thermodynamic equilibrium were used to calculate in situ aerosol pH.

$$\text{pH} = -\log[\gamma_{H_{aq}^+} \times n_{H_{aq}^+}/(V_{aq}/1000)] \quad (3)$$

$\gamma_{H_{aq}^+}$: activity coefficient of H_{aq}^+
$n_{H_{aq}^+}$: moles of H_{aq}^+
V_{aq}: total volume of the aqueous phase (cm^3)

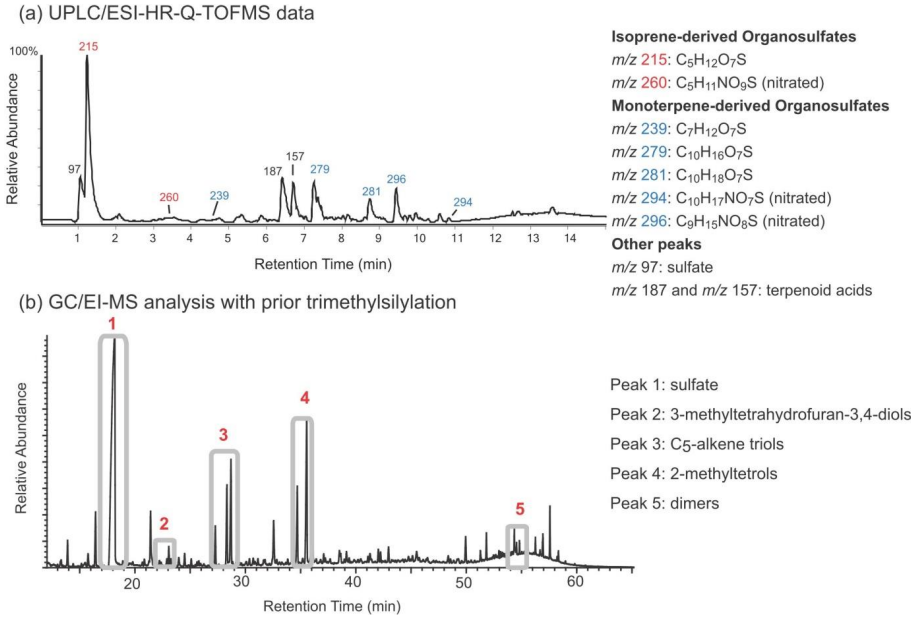

Fig. 2. Representative **(a)** UPLC/ESI-HR-Q-TOFMS base peak chromatogram and **(b)** GC/EI-MS total ion chromatogram of the $PM_{2.5}$ sample collected at YRK on 27 June 2010 under high-SO_2 conditions, showing isoprene-derived SOA tracers were major SOA constituents detected at this site during summertime.

3 Results and discussion

As the SO_2 conditional sampling and NH_3 conditional sampling experiments were two independent experiments, samples collected from SO_2 and NH_3 conditional sampling experiments could not be inter-compared for the following reasons:

1. SO_2 conditional sampling experiments were conducted 25 June 2010–14 July 2010. During this time, $PM_{2.5}$ sample collections were determined by the ambient SO_2 mixing ratios. Thus, only high- and low-SO_2 samples collected on the same day (as a paired sample) could be compared, since other variables, including NH_3, were not constrained.

2. Similarly, NH_3 conditional sampling experiments were conducted 29 July 2010–6 August 2010, and only the ambient NH_3 mixing ratios determined when the high-volume samplers were operated. We considered high- and low-NH_3 samples collected on the same day as a paired sample to distinguish the effects of ambient NH_3.

3.1 Identification and quantification of isoprene SOA tracers at YRK

UPLC/(–)ESI-HR-Q-TOFMS and GC/EI-MS with prior trimethylsilylation were used to identify and quantify isoprene SOA tracers in the $PM_{2.5}$ samples collected from the YRK site. Figure 2 shows a typical base peak chromatogram (BPC) from UPLC/(–)ESI-HR-Q-TOFMS analysis, and a typical total ion chromatogram (TIC) from GC/EI-MS analysis for a representative $PM_{2.5}$ sample collected on 27 June 2010 under the high-SO_2 sampling scenario. Overall, most of the major peaks identified from the filter samples could be attributed to BSOA tracers, which have been confirmed by prior chamber studies (Surratt et al., 2008, 2010; Lin et al., 2012). The IEPOX-derived organosulfate ($[M–H]^-$ ion at m/z 215) was the most abundant compound detected by the UPLC/(–)ESI-HR-Q-TOFMS technique. Other base peak ions displayed in the BPC correspond to monoterpene-derived organosulfates (e.g., $[M–H]^-$ ions at m/z 239, 279, and 281) (Surratt et al., 2008), nitrooxy (or nitrated) organosulfates derived from both isoprene (e.g., $[M–H]^-$ ion at m/z 260) and monoterpenes (e.g., $[M–H]^-$ ions at m/z 294 and 296) (Surratt et al., 2008), and terpenoic acids (e.g., $[M–H]^-$ ions at m/z 157 and 187) (Yasmeen et al., 2011). For the TIC from GC/EI-MS analysis, the most abundant peak (labeled as Peak 1) was identified as bis(trimethylsilyl) sulfate based on the NIST MS library search. This peak, which likely originates from the extracted particle sulfate content after trimethylsilylation, was also observed by Jaoui et al. (2012) in the samples collected from chamber studies under conditions of pre-seeded ammonium sulfate aerosol and SO_2 oxidation that forms sulfuric acid. Other major peaks detected could be attributed to isoprene low-NO_x SOA tracers, including 3-MeTHF-3,4-diols (two isomers grouped as Peak 2), C_5-alkene triols (three isomers grouped as Peak 3), and 2-methyltetrols (two isomers grouped Peak 4). Strong signal intensity of C_5-alkene triols and 2-methyltetrols in the TIC, as well as the IEPOX-derived

organosulfate in the BPC from the UPLC/(–)ESI-HR-Q-TOFMS technique, shows the atmospheric significance of IEPOX chemistry leading to SOA formation in this region.

SOA tracer compounds were quantified with authentic or surrogate standards. Field blanks were collected during the field study, and subsequently analyzed to subtract background signals from all aerosol samples for quantification. The average mass concentrations of isoprene low-NO_x and high-NO_x SOA tracers measured under high- and low-SO_2 conditions in this study are shown in Table 2. For high SO_2 conditional samples, the average mass concentration of isoprene low-NO_x tracers, including 2-methyltetrols, C_5-alkene triols, 3-MeTHF-3,4-diols, as well as IEPOX-derived organosulfate (m/z 215), were higher than those of the corresponding paired low SO_2 conditional samples ($p = 0.012$). The differences of isoprene high-NO_x (MAE-derived) SOA tracers between high- and low-SO_2 conditions were not as significant ($p = 0.754$). This observation provides evidence for isoprene SOA formation from IEPOX chemistry being enhanced under a high-SO_2 environment. The enhancement of isoprene SOA formation, especially for the identified isoprene low-NO_x SOA tracers, can be explained by the oxidation of SO_2 producing sulfuric acid that provides aerosol acidity to enhance the rate of heterogeneous oxirane ring-opening reactions when the gas-phase IEPOX is taken up by preexisting acidic aerosol surfaces (Edney et al., 2005; Surratt et al., 2010; Lin et al., 2012). Moreover, the enhancement of IEPOX chemistry could also be explained by the increased aerosol sulfate concentrations under high-SO_2 conditions (Table 1). The hygroscopic nature of the particle sulfate could have provided a wet aerosol surface that facilitated the IEPOX uptake and lead to SOA formation. In order to clarify the role of SO_2, correlations between aerosol acidity, particle sulfate loadings and isoprene low-NO_x SOA tracers are discussed in subsequent sections of this manuscript. It is noteworthy that the previous detection of particle-phase IEPOX in Chan et al. (2010b), which was characterized as m/z 262 with prior trimethylsilylation using GC/EI-MS analysis, has been shown to be a misidentification of 3-MeTHF-3, 4-diols (Lin et al., 2012). This is confirmed through organic synthesis of both IEPOX and 3-MeTHF-3, 4-diols authentic standards (Zhang et al., 2012). The concentrations of 3-MeTHF-3, 4-diols detected in this study were estimated ranging from non-detactable (n.d.) to 35 ng m^{-3}, which were comparable to the reported particle-phase IEPOX in Chan et al. (2010b) (n.d. to 24 ng m^{-3}).

One possible source of uncertainty regarding quantification of 2-methyltetrols and 2-methylglyceric acid should be noted. These two tracers could possibly be overestimated due to the hydrolysis and derivatization of IEPOX- and MAE-derived organosulfates upon trimethylsilylation. To evaluate the extent of this effect, we analyzed sodium octyl sulfate using GC/MS with prior trimethylsilylation, and compared the results to octanol with trimethylsilylation. Sodium octyl sulfate and octanol were used here as surrogates owing to the lack of authentic standards for IEPOX- and MAE-derived organosulfates, as well as their hydrolyzed products (i.e., 2-methyltetrols and 2-methylglyceric acid). The results indicate ~ 1.6 % octyl sulfate was hydrolyzed during the process of trimethylsilylation. This implies likely only a small fraction of IEPOX- or MAE-derived organosulfates would be hydrolyzed during the same analytical process and quantified as 2-methyltetrols and 2-methylglyceric acid. However, while isoprene-derived organosulfates are more highly substituted with electron withdrawing groups, the potential limitation of using octyl sulfate as a proxy should be noted, since octyl sulfate is a primary sulfate with no substitution on adjacent carbons. Additionally, the MAE-derived organosulfate (detected as the $[M–H]^-$ ion at m/z 199) produced a MS/MS spectrum (Fig. 1S, see Supplement) consistent with that recently shown by Safi Shalamzari et al. (2013).

Table 2. Isoprene SOA tracers quantified in $PM_{2.5}$ samples (ng m^{-3}) collected under high- and low-SO_2 conditions.

Isoprene low-NO_x SOA tracers (IEPOX-derived SOA tracers)	High SO_2	Low SO_2
2-methyltetrols	316.7 ± 21.5	283.9 ± 33.7
C_5 alkene triols	319.6 ± 32.4	258.8 ± 33.0
3-MeTHF-3,4-diols	11.4 ± 1.4	7.5 ± 1.4
Dimers	1.3 ± 0.3	1.2 ± 0.3
IEPOX-derived organosulfate (m/z 215)	107.3 ± 14.8	92.1 ± 19.5
Organosulfate of dimers (m/z 333)	2.7 ± 0.5	2.7 ± 0.7
Σ IEPOX SOA tracers/OM [a]	13.3 %	11.9 %
Isoprene high-NO_x SOA tracers (MAE-derived SOA tracers)		
2-MG	7.4 ± 0.8	8.6 ± 1.5
MAE-derived organosulfate (m/z 199)	11.9 ± 0.9	11.8 ± 2.2
Σ MAE SOA tracers/OM [b]	0.34 %	0.36 %

[a] Paired t test ($n = 16$); $p = 0.012$*.
[b] Paired t test ($n = 16$); $p = 0.754$.

The average mass concentrations of isoprene SOA tracers measured under high- and low-NH_3 conditions are shown in Table 3. Organosulfate species, such as the IEPOX-derived organosulfate (m/z 215), the organosulfate derivative of the IEPOX-derived dimers (m/z 333), and MAE-derived organosulfate (m/z 199) were more abundant under low-NH_3 conditions. Other tracer compounds, however, have higher mass concentrations detected under high-NH_3 conditions, which might coincide with the higher average solar radiation under high NH_3 conditional sampling (Table 1). Figure 3 shows correlations between isoprene-derived organosulfates. Interestingly, strong correlations between the IEPOX-derived organosulfate (m/z 215) and the organosulfate derivatives of the IEPOX-derived dimers

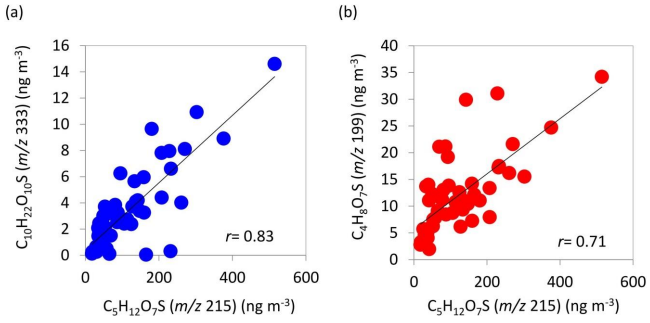

Fig. 3. Correlations between isoprene-derived organosulfates: **(a)** correlations between IEPOX-derived organosulfate (m/z 215) and organosulfate derivatives of IEPOX-derived dimers (m/z 333) support the common isoprene low-NO_x pathway and formation mechanisms of these two tracers. **(b)** Correlations between the IEPOX-derived organosulfate (m/z 215) and the MAE-derived organosulfate (m/z 199) suggest similar limiting factors for organosulfate formation, as these two species have been known to form from isoprene photooxidation through low-NO_x and high-NO_x pathways, respectively.

(m/z 333) ($r = 0.83$) support the common pathway and formation mechanisms of these two tracers, as shown in Fig. 1. In addition, strong correlations ($r = 0.71$) were observed between the IEPOX-derived organosulfate (m/z 215) and the MAE-derived organosulfate (m/z 199), suggesting similar formation behaviors or limiting factors, since these two species are known to form from different NO_x-dependent pathways as shown in Fig. 1. Reactive uptake of epoxide precursors followed by particle-phase oxirane ring-opening reactions appears to be a common mechanism for both low-NO_x and high-NO_x isoprene SOA formation pathways, although yielding distinct SOA composition. Notably, the detected isoprene low-NO_x SOA tracers were higher during the NH_3 conditional sampling period (late July to early August) than the SO_2 conditional sampling period (late June to mid-July), likely due to the change of meteorological conditions. For example, a higher average temperature during the NH_3 conditional sampling period might lead to higher isoprene emissions, as well as faster photochemical processes for isoprene SOA formation. In contrast, the isoprene high-NO_x SOA tracers remained constant between the two sampling periods. This could be explained by the NO-limited isoprene SOA formation pathway that occurs once the NO levels in the environment are consumed, resulting in the low-NO_x (RO_2+HO_2) chemistry becoming the dominant pathway in the atmosphere, while isoprene is still continuously emitted during daytime.

Temporal variations of isoprene low-NO_x and high-NO_x SOA tracers compared to OM are shown in Figs. 4 and 5, respectively. On most days, IEPOX- and MAE-derived SOA tracers track well with the OM mass loadings. The r values range from 0.40–0.68 for IEPOX-derived SOA tracers and 0.17–0.69 for MAE-derived SOA tracers. Weak correlations occur under high NH_3 conditional sampling events for both IEPOX- and MAE-derived SOA tracers. It is worth noting that the sum of IEPOX-derived SOA tracers contributed substantially (12–19 %) to the total organic matter (OM) in the $PM_{2.5}$ samples collected at this site, showing the atmospheric abundance of the isoprene low-NO_x (or IEPOX-derived) SOA that originates from a single source and pathway (Tables 2 and 3). OM was estimated as OC × 1.8 here for summertime aerosols (Simon et al., 2011). To examine whether or not the differences of isoprene SOA formation between high and low SO_2 or NH_3 conditional sampling protocols were significant, paired-t tests were performed. The results of the paired-t tests indicate that the enhancement of IEPOX-derived SOA is statistically significant ($p = 0.012$) under high-SO_2 conditions. No significant enhancement of the sum of isoprene SOA tracers was observed for high or low NH_3 conditional samples ($p = 0.830$).

Table 3. Isoprene SOA tracers quantified in $PM_{2.5}$ samples (ng m^{-3}) collected under high- and low-NH_3 conditions.

Isoprene low-NO_x SOA tracers (IEPOX-derived SOA tracers)	High NH_3	Low NH_3
2-methyltetrols	572.7 ± 82.6	414.0 ± 83.6
C-5 alkene triols	524.1 ± 92.6	482.0 ± 133.5
3-MeTHF-3,4-diols	19.0 ± 3.5	14.4 ± 3.8
Dimers	2.1 ± 0.6	2.4 ± 0.9
IEPOX-derived organosulfate (m/z 215)	104.3 ± 40.0	196.5 ± 48.9
Organosulfate of dimers (m/z 333)	3.1 ± 1.0	4.8 ± 1.5
Σ IEPOX SOA tracers/OM [a]	19.1 %	18.6 %
Isoprene high-NO_x SOA tracers (MAE-derived SOA tracers)		
2-MG	9.9 ± 1.3	7.6 ± 1.3
MAE-derived organosulfate (m/z 199)	9.9 ± 2.3	13.6 ± 3.2
Σ MAE SOA tracers/OM [b]	0.31 %	0.37 %

[a] Paired t test ($n = 9$); $p = 0.830$.
[b] Paired t test ($n = 9$); $p = 0.506$.

3.2 Comparisons of continuous inorganic measurements to filter-based IC data

Figure 6 shows comparisons of continuous inorganic measurement to filter-based measurements in this study. Time-weighted average of continuous inorganic data was compared to the IC data from filter samples. Strong correlations were observed for particle NH_4^+ ($r = 0.85$) and SO_4^{2-} ($r = 0.79$) concentrations from two data sets. The correlation for particle NO_3^- concentrations was ($r = 0.49$) weak, possibly due to low concentrations throughout the study and artifacts in both the filter and continuous measurements.

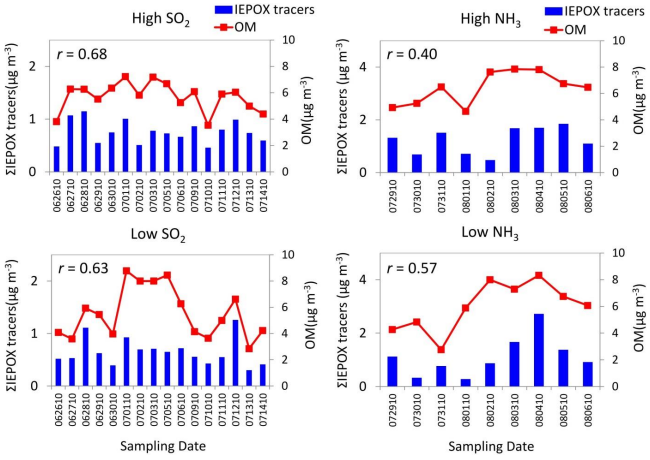

Fig. 4. Temporal variations of low-NO_x SOA tracers and OM.

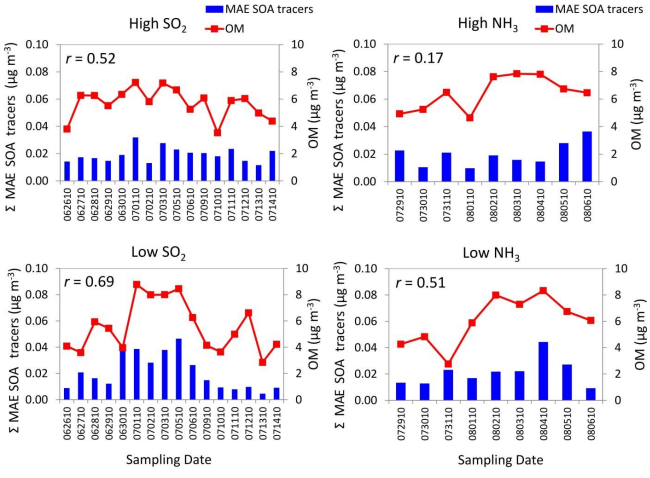

Fig. 5. Temporal variations of isoprene high-NO_x SOA tracers and OM.

3.3 Ambient aerosol acidity and isoprene SOA tracers

To estimate aerosol acidity of collected $PM_{2.5}$ samples, the degree of neutralization was calculated as the molar ratio of ammonium to the sum of sulfate and nitrate ($[NH_4^+]/(2\times[SO_4^{2-}]+[NO_3^-])$. Acidic aerosols are characterized with neutralization degrees less than unity, while neutralization degrees greater than unity imply the samples are neutralized. Figure 7 compares the degree of neutralization for $PM_{2.5}$ samples collected in this study calculated from on-line continuous inorganic measurements and filter-based IC data. In general, most of the aerosol samples have been fully neutralized. However, the frequency distribution from filter-based data shows that most of the samples had the neutralization degree close to unity, while data from continuous inorganic measurements had a more broad distribution. Since filter samples could have absorbed the ambient acidic or basic gases that lead to neutralization of aerosol samples over time

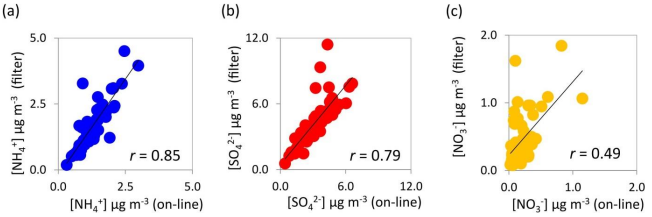

Fig. 6. Comparisons of on-line continuous particle analyzer data and filter-based IC measurements: **(a)** NH_4^+, **(b)** SO_4^{2-}, **(c)** NO_3^-.

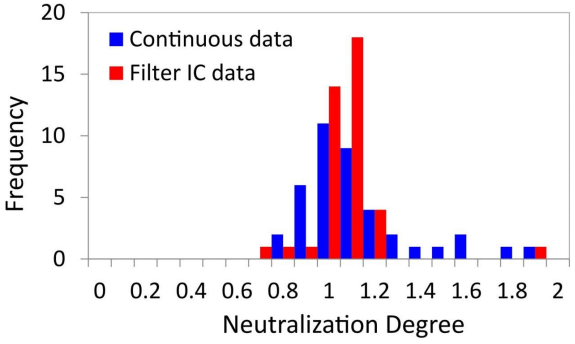

Fig. 7. Frequency distribution of the neutralization degree from aerosol samples calculated by on-line continuous particle analyzer data (blue) and filter-based IC data (red).

during the sampling period, to capture the more representative aerosol acidity, continuous inorganic data were used for further data analysis.

Figure 8 shows the distribution of aerosol samples grouping based on sampling conditions. SO_2 conditional samples are acidic, while NH_3 conditional samples are more neutralized. Figure 9 shows the result from E-AIM II modeling. In situ aerosol pH can only be calculated in very few cases due to the neutralized characteristics of aerosol samples. In addition, some of the samples, although not fully neutralized, were modeled as no liquid water content (LWC) under given RH conditions. More specifically, the amount of water (LWC) in an aerosol particle calculated using the E-AIM Model II system (H^+-NH_4^+-SO_4^{2-}-NO_3^--H_2O) is dependent on the inorganic materials (electrolytes) present, the ambient relative humidity, and temperature. Although there were some other high RH episodes observed during the sampling period (with RH > 0.8), these samples in fact have been fully neutralized ($[H^+]_{free} < 0$), and thus have to be excluded from the data set in the first place, since a charge imbalance in the ionic composition of the system is not allowed for the model input. Thus, aerosol pH could not be calculated for those samples either. As a result, only very limited number of samples could be modeled using this approach. Only 3 samples (out of 50) could be modeled for their in situ aerosol pH, and the average was found to be 1.71, ranging from 1.69 to 1.75. However, the E-AIM model in this study was run under the assumption of no interaction between the organic

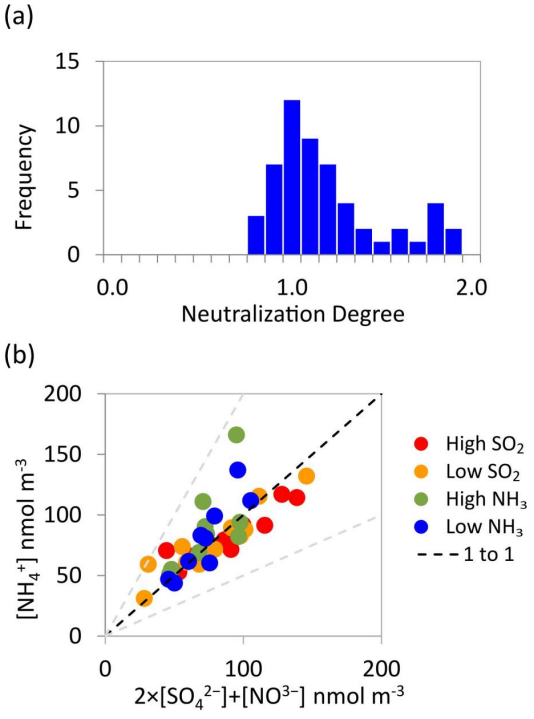

Fig. 8. (a) Frequency distribution of the neutralization degree from aerosol samples **(b)** NH_4^+ to SO_4^{2-} plus NO_3^- ratios.

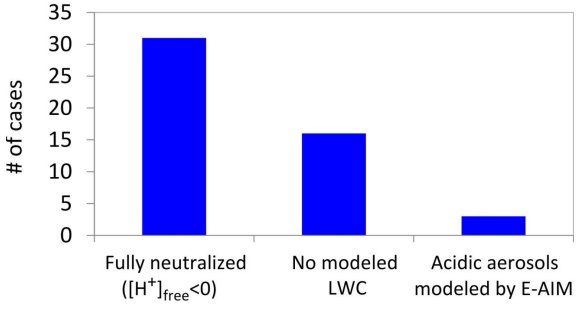

Fig. 9. E-AIM II modeling: in situ aerosol pH can only be calculated in very few cases (3 out of 50) in our samples. A total 31 aerosol samples were calculated as fully neutralized ($[H^+]_{free} < 0$) that could not be modeled by E-AIM II. Altogether, 16 samples were shown as no modeled LWC.

phase and the inorganic phase. In a recent study by Smith et al. (2012), isoprene-derived secondary organic materials have been shown to mix miscibly with aqueous ammonium sulfate, and the resultant mixture shifted efflorescence and deliquescence points of pure ammonium sulfate. As a result, the modeling results could be inaccurate under this assumption, and thus did not capture the actual particle LWC.

Figures 10 and 11 show the correlations between the neutralization degree and the sum of isoprene low-NO_x (or IEPOX-derived) and high-NO_x (or MAE-derived) SOA tracers, respectively. For IEPOX-derived SOA, the results show

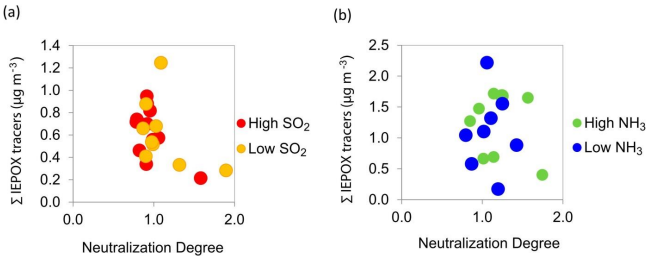

Fig. 10. Effects of aerosol acidity on IEPOX-derived SOA formation: **(a)** SO_2 conditional samples; **(b)** NH_3 conditional samples. The sum of IEPOX-derived SOA tracers was enhanced with less-neutralized (i.e., more acidic) aerosols for SO_2 conditional samples, but no clear associations were observed for NH_3 conditional samples.

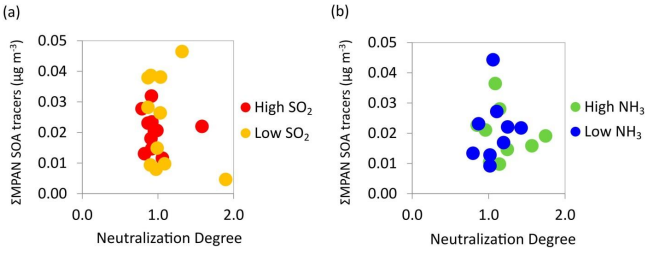

Fig. 11. Effects of aerosol acidity on isoprene high-NOx SOA formation: **(a)** SO_2 conditional samples; **(b)** NH_3 conditional samples. No clear associations between aerosol acidity and the sum of MAE-derived SOA tracers were observed for either SO_2 or NH_3 conditional samples.

that the tracer compounds were weakly enhanced with less-neutralized aerosols, but no clear associations were observed for NH_3 conditional samples. For MAE-derived SOA, no clear associations were observed for either SO_2 or NH_3 conditional samples. This could be due to most of the aerosol samples being fully neutralized. Notably, prior chamber work has shown that under high-NO_x conditions no enhancement in SOA mass was observed due to the presence of acidified sulfate seed aerosol, whereas under low-NO_x conditions SOA mass was enhanced due to the presence of acidified sulfate seed aerosol (Surratt et al., 2006). Furthermore, the aerosol samples could have formed upwind of the sampling site, and thus were associated to a more aged and regional (background) aerosol type. Thus, distinguishing weak correlations from meteorological effects on measured isoprene SOA levels is challenging, since the isoprene SOA might have been formed upwind, but not formed locally. It should also be noted that the history of ambient aerosol acidity is complicated. The aerosol could be neutralized on average with time, but start as an acidic aerosol that has already provided sufficient acidity to allow significant IEPOX processing. Our findings are in agreement with Tanner et al. (2009), who previously reported that at the YRK site no consistent positive correlations were found between changes in OC

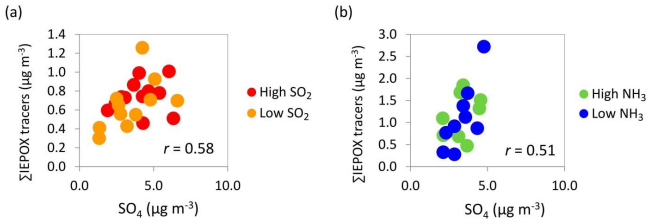

Fig. 12. Correlations between the sum of IEPOX SOA tracers and the particle sulfate loadings: **(a)** SO_2 conditional samples; **(b)** NH_3 conditional samples. Positive correlations were observed for both SO_2 and NH_3 conditional samples, indicating a role of particle sulfate loadings for providing surface area that limits the IEPOX uptake and forming SOA tracers.

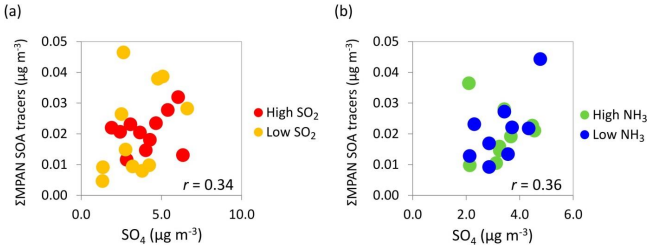

Fig. 13. Correlations between the sum of MAE-derived SOA tracers and the particle sulfate loadings: **(a)** SO_2 conditional samples; **(b)** NH_3 conditional samples. Positive correlations were observed for both SO_2 and NH_3 conditional samples, suggesting surface area could be a limiting factor that modulates isoprene high-NO_x SOA formation.

or TC levels and aerosol acidity, which was estimated by nitrate-corrected ammonium-to-sulfate ratios, even with time lag up to 6 h. Aerosol acidity at this site is relatively low due to nearby agricultural sources of NH_3. In addition, recent research by Liggio et al. (2011) reported that the rate of aerosol neutralization by NH_3 uptake is significantly reduced in the presence of ambient organic gases on timescales ~ 10 min to several hours, while acidic aerosol mixed with organic-free air and NH_3 was neutralized on a timescale < 1 min. This reduction in NH_3 uptake was concurrent with an increase in the amount of particle-phase organics. Thus, our NH_3 conditional sampling approaches might not be able to capture the neutralization effects on aerosol acidity and isoprene SOA formation, since this would not be an instantaneous process in the ambient environment.

3.4 Particle sulfate loadings and isoprene SOA tracers

Figures 12 and 13 show correlations between isoprene low-NO_x and high-NO_x SOA tracers and the particle sulfate loadings, with $r = 0.51$–0.58 for IEPOX-derived SOA tracers and $r = 0.34$–0.36 for MAE-derived SOA tracers, respectively. Figure 14 shows correlations between the sum of isoprene SOA tracers (combining IEPOX- and MAE-derived SOA) and particle SO_4^{2-} loadings for all $PM_{2.5}$ samples collected

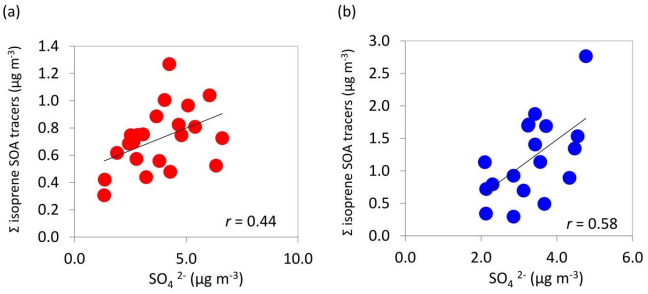

Fig. 14. Correlations between the sum of isoprene SOA tracers (combining IEPOX- and MAE-derived SOA) and the particle sulfate loadings for all $PM_{2.5}$ samples collected in this study from **(a)** 25 June to 14 July 2010 (SO_2 conditional sampling period) and **(b)** 29 July 2010 to 6 August 2010 (NH_3 conditional sampling period).

during SO_2 conditional sampling period ($r = 0.44$) and the NH_3 conditional sampling period ($r = 0.58$) in this study. Positive correlations were observed for all conditions. These condition-independent correlations may suggest that aerosol sulfate could serve as the surface accommodation factor that facilitates the reactive uptake of IEPOX onto preexisting aerosols. Although acidified sulfate aerosol has been demonstrated to enhance heterogeneous isoprene SOA formation (Surratt et al., 2007b, 2010), laboratory studies are lacking that systematically examine the effect of varying surface area of preexisting aerosol on isoprene SOA formation as a function of liquid water content, aerosol acidity, and chemical composition. More work is needed to understand if this is a surface- or bulk-limited process and how this changes with environmental conditions.

4 Conclusions

Analyses of $PM_{2.5}$ samples collected from the rural southeastern US by off-line chromatography coupled with mass spectrometry techniques show substantial contributions (12–19 %) of isoprene low-NO_x SOA tracers to organic aerosol mass, revealing the importance for heterogeneous chemistry of IEPOX in this region. Conditional sampling approaches employed in this study indicate that IEPOX-derived SOA formation is enhanced under higher SO_2 conditions ($p = 0.012$). In contrast, conditional sampling did not show significant influence of NH_3 levels on low-NO_x isoprene SOA concentrations. Thus, it is possible that the effects (or degree) of NH_3 neutralization were masked by other confounding factors or atmospheric processes occurring simultaneously. Particle sulfate loadings have moderate positive correlations with the sum of isoprene SOA tracers for all conditions, suggesting a role of surface- or bulk-limited chemistry for isoprene SOA formation.

Weak correlations between isoprene SOA tracers and aerosol acidity could be attributed to the fact that information is lacking about the history of the ambient aerosol acidity. Evaporation of volatile particle constituents, such as nitrates, would affect the estimate of aerosol acidity, although NO_3^- concentrations were generally too low to make a big difference in the neutralization calculation. In addition, during the volatilization process it remains uncertain if this is primarily HNO_3 or HNO_3 plus NH_3 leaving the filters. The latter would not have any effect on acidity.

Since very few samples could be modeled using E-AIM II, our ability to elucidate potential effects of aqueous-phase chemistry on isoprene SOA formation is quite limited. Regional-scale transport could have brought isoprene SOA formed upwind that masked the effects of aerosol acidity. As a result, future work is needed to differentiate the effects of enhanced BSOA formation from regional-scale transport and aqueous-phase chemistry.

Supplementary material related to this article is available online at: http://www.atmos-chem-phys.net/13/8457/2013/acp-13-8457-2013-supplement.pdf.

Acknowledgements. This research was funded by Electric Power Research Institute (EPRI). UPLC/ESI-HR-Q-TOFMS analyses were conducted in the UNC-CH Biomarker Mass Facility located within the Department of Environmental Sciences and Engineering, which is a part of the UNC-CH Center for Environmental Health and Susceptibility supported by NIEHS (Grant 5P20-ES10126). Y.-H. Lin acknowledges a Dissertation Completion Fellowship from the UNC Graduate School. Avram Gold and Zhenfa Zhang (Univ. of North Carolina at Chapel Hill) are gratefully acknowledged for the synthesis of 3-MeTHF-3,4-diols standards.

Edited by: F. Keutsch

References

Chan, A. W. H., Chan, M. N., Surratt, J. D., Chhabra, P. S., Loza, C. L., Crounse, J. D., Yee, L. D., Flagan, R. C., Wennberg, P. O., and Seinfeld, J. H.: Role of aldehyde chemistry and NO_x concentrations in secondary organic aerosol formation, Atmos. Chem. Phys., 10, 7169–7188, doi:10.5194/acp-10-7169-2010, 2010a.

Chan, M. N., Surratt, J. D., Claeys, M., Edgerton, E. S., Tanner, R. L., Shaw, S. L., Zheng, M., Knipping, E. M., Eddingsaas, N. C., and Wennberg, P. O.: Characterization and quantification of isoprene-derived epoxydiols in ambient aerosol in the southeastern United States, Environ. Sci. Technol., 44, 4590–4596, 2010b.

Chan, M. N., Surratt, J. D., Chan, A. W. H., Schilling, K., Offenberg, J. H., Lewandowski, M., Edney, E. O., Kleindienst, T. E., Jaoui, M., Edgerton, E. S., Tanner, R. L., Shaw, S. L., Zheng, M., Knipping, E. M., and Seinfeld, J. H.: Influence of aerosol acidity on the chemical composition of secondary organic aerosol from β-caryophyllene, Atmos. Chem. Phys., 11, 1735–1751, doi:10.5194/acp-11-1735-2011, 2011.

Chung, S. H. and Seinfeld, J. H.: Global distribution and climate forcing of carbonaceous aerosols, J. Geophys. Res., 107, 4407, doi:10.1029/2001JD001397, 2002.

Claeys, M., Graham, B., Vas, G., Wang, W., Vermeylen, R., Pashynska, V., Cafmeyer, J., Guyon, P., Andreae, M. O., and Artaxo, P.: Formation of secondary organic aerosols through photooxidation of isoprene, Science, 303, 1173–1176, 2004.

Clegg, S. L., Brimblecombe, P., and Wexler, A. S.: Thermodynamic model of the system H^+-NH_4^+-SO_4^{2-}-NO_3^--H_2O at tropospheric temperatures, J. Phys. Chem. A, 102, 2137–2154, 1998.

Eddingsaas, N. C., VanderVelde, D. G., and Wennberg, P. O.: Kinetics and products of the acid-catalyzed ring-opening of atmospherically relevant butyl epoxy alcohols, J. Phys. Chem. A, 114, 8106–8113, 2010.

Edgerton, E. S., Hartsell, B. E., Saylor, R. D., Jansen, J. J., Hansen, D. A., and Hidy, G. M.: The Southeastern Aerosol Research and Characterization Study: Part II. Filter-based measurements of fine and coarse particulate matter mass and composition, J. Air Waste Manage., 55, 1527–1542, 2005.

Edgerton, E. S., Hartsell, B. E., and Jansen, J. J.: Mercury speciation in coal-fired power plant plumes observed at three surface sites in the southeastern US, Environ. Sci. Technol., 40, 4563–4570, 2006a.

Edgerton, E. S., Hartsell, B. E., Saylor, R. D., Jansen, J. J., Hansen, D. A., and Hidy, G. M.: The Southeastern Aerosol Research and Characterization Study, part 3: Continuous measurements of fine particulate matter mass and composition, J. Air Waste Manage., 56, 1325–1341, 2006b.

Edgerton, E. S., Saylor, R. D., Hartsell, B. E., Jansen, J. J., and Alan Hansen, D.: Ammonia and ammonium measurements from the southeastern United States, Atmos. Environ., 41, 3339–3351, 2007.

Edney, E., Kleindienst, T., Jaoui, M., Lewandowski, M., Offenberg, J., Wang, W., and Claeys, M.: Formation of 2-methyl tetrols and 2-methylglyceric acid in secondary organic aerosol from laboratory irradiated isoprene/NO_x/SO_2/air mixtures and their detection in ambient $PM_{2.5}$ samples collected in the eastern United States, Atmos. Environ., 39, 5281–5289, 2005.

Gao, S., Surratt, J. D., Knipping, E. M., Edgerton, E. S., Shahgholi, M., and Seinfeld, J. H.: Characterization of polar organic components in fine aerosols in the southeastern United States: Identity, origin, and evolution, J. Geophys. Res., 111, D14314, doi:10.1029/2005jd006601, 2006.

Goldstein, A. H., Koven, C. D., Heald, C. L., and Fung, I. Y.: Biogenic carbon and anthropogenic pollutants combine to form a cooling haze over the southeastern United States, P. Natl. Acad. Sci. USA, 106, 8835–8840, 10.1073/pnas.0904128106, 2009.

Hallquist, M., Wenger, J. C., Baltensperger, U., Rudich, Y., Simpson, D., Claeys, M., Dommen, J., Donahue, N. M., George, C., Goldstein, A. H., Hamilton, J. F., Herrmann, H., Hoffmann, T., Iinuma, Y., Jang, M., Jenkin, M. E., Jimenez, J. L., Kiendler-Scharr, A., Maenhaut, W., McFiggans, G., Mentel, Th. F., Monod, A., Prévôt, A. S. H., Seinfeld, J. H., Surratt, J. D., Szmigielski, R., and Wildt, J.: The formation, properties and impact of secondary organic aerosol: current and emerging issues, Atmos. Chem. Phys., 9, 5155–5236, doi:10.5194/acp-9-5155-2009, 2009.

Hansen, D. A., Edgerton, E. S., Hartsell, B. E., Jansen, J. J., Kandasamy, N., Hidy, G. M., and Blanchard, C. L.: The southeastern

aerosol research and characterization study: Part 1-overview, J. Air Waste Manage., 53, 1460–1471, 2003.

Henze, D. K. and Seinfeld, J. H.: Global secondary organic aerosol from isoprene oxidation, Geophys. Res. Lett, 33, L09812, doi:10.1029/2006GL025976, 2006.

Huang, X., Qiu, R., Chan, C. K., and Ravi Kant, P.: Evidence of high $PM_{2.5}$ strong acidity in ammonia-rich atmosphere of Guangzhou, China: Transition in pathways of ambient ammonia to form aerosol ammonium at $[NH_4^+]/[SO_4^{2-}] = 1.5$, Atmos. Res., 99, 488–495, 2011.

Huntzicker, J. J., Cary, R. A., and Ling, C. S.: Neutralization of sulfuric acid aerosol by ammonia, Environ. Sci. Technol., 14, 819–824, 1980.

Iinuma, Y., Böge, O., Gnauk, T., and Herrmann, H.: Aerosol-chamber study of the α-pinene/O_3 reaction: influence of particle acidity on aerosol yields and products, Atmos. Environ., 38, 761–773, 2004.

Iinuma, Y., Müller, C., Berndt, T., Böge, O., Claeys, M., and Herrmann, H.: Evidence for the existence of organosulfates from β-pinene ozonolysis in ambient secondary organic aerosol, Environ. Sci. Technol., 41, 6678–6683, 2007.

Iinuma, Y., Böge, O., Kahnt, A., and Herrmann, H.: Laboratory chamber studies on the formation of organosulfates from reactive uptake of monoterpene oxides, Phys. Chem. Chem. Phys., 11, 7985–7997, 2009.

Jaoui, M., Kleindienst, T. E., Offenberg, J. H., Lewandowski, M., and Lonneman, W. A.: SOA formation from the atmospheric oxidation of 2-methyl-3-buten-2-ol and its implications for $PM_{2.5}$, Atmos. Chem. Phys., 12, 2173–2188, doi:10.5194/acp-12-2173-2012, 2012.

Kanakidou, M., Seinfeld, J. H., Pandis, S. N., Barnes, I., Dentener, F. J., Facchini, M. C., Van Dingenen, R., Ervens, B., Nenes, A., Nielsen, C. J., Swietlicki, E., Putaud, J. P., Balkanski, Y., Fuzzi, S., Horth, J., Moortgat, G. K., Winterhalter, R., Myhre, C. E. L., Tsigaridis, K., Vignati, E., Stephanou, E. G., and Wilson, J.: Organic aerosol and global climate modelling: a review, Atmos. Chem. Phys., 5, 1053–1123, doi:10.5194/acp-5-1053-2005, 2005.

Kleindienst, T. E., Jaoui, M., Lewandowski, M., Offenberg, J. H., Lewis, C. W., Bhave, P. V., and Edney, E. O.: Estimates of the contributions of biogenic and anthropogenic hydrocarbons to secondary organic aerosol at a southeastern US location, Atmos. Environ., 41, 8288–8300, 2007.

Liggio, J., Li, S. M., Vlasenko, A., Stroud, C., and Makar, P.: Depression of ammonia uptake to sulfuric acid aerosols by competing uptake of ambient organic gases, Environ. Sci. Technol., 45, 2790–2796, 2011.

Lin, Y.-H., Zhang, Z., Docherty, K. S., Zhang, H., Budisulistiorini, S. H., Rubitschun, C. L., Shaw, S. L., Knipping, E. M., Edgerton, E. S., Kleindienst, T. E., Gold, A., and Surratt, J. D.: Isoprene epoxydiols as precursors to secondary organic aerosol formation: Acid-catalyzed reactive uptake studies with authentic compounds, Environ. Sci. Technol., 46, 250–258, doi:10.1021/es202554c, 2012.

Lin, Y.-H., Zhang, H., Pye, H. O. T., Zhang, Z., Marth, W. J., Park, S., Arashiro, M., Cui, T., Budisulistiorini, S. H., Sexton, K. G., Vizuete, W., Xie, Y., Luecken, D. J., Piletic, I. R., Edney, E. O., Bartolotti, L. J., Gold, A., and Surratt, J. D.: Epoxide as a precursor to secondary organic aerosol formation from isoprene photooxidation in the presence of nitrogen oxides, P. Natl. Acad. Sci. USA, 110, 6718–6723, doi:10.1073/pnas.1221150110, 2013.

McMurry, P. H., Takano, H., and Anderson, G. R.: Study of the ammonia (gas)-sulfuric acid (aerosol) reaction rate, Environ. Sci. Technol., 17, 347–352, doi:10.1021/es00112a008, 1983.

Minerath, E. C., Schultz, M. P., and Elrod, M. J.: Kinetics of the reactions of isoprene-derived epoxides in model tropospheric aerosol solutions, Environ. Sci. Technol., 43, 8133–8139, 2009.

Offenberg, J. H., Lewandowski, M., Edney, E. O., Kleindienst, T. E., and Jaoui, M.: Influence of aerosol acidity on the formation of secondary organic aerosol from biogenic precursor hydrocarbons, Environ. Sci. Technol., 43, 7742–7747, 2009.

Safi Shalamzari, M., Ryabtsova, O., Kahnt, A., Vermeylen, R., Hérent, M.-F., Quetin-Leclercq, J., Van der Veken, P., Maenhaut, W., and Claeys, M.: Mass spectrometric characterization of organosulfates related to secondary organic aerosol from isoprene, Rapid Commun. Mass Sp., 27, 784–794, doi:10.1002/rcm.6511, 2013.

Saylor, R. D., Edgerton, E. S., Hartsell, B. E., Baumann, K., and Hansen, D. A.: Continuous gaseous and total ammonia measurements from the southeastern aerosol research and characterization (SEARCH) study, Atmos. Environ., 44, 4994–5004, 2010.

Simon, H., Bhave, P. V., Swall, J. L., Frank, N. H., and Malm, W. C.: Determining the spatial and seasonal variability in OM/OC ratios across the US using multiple regression, Atmos. Chem. Phys., 11, 2933–2949, doi:10.5194/acp-11-2933-2011, 2011.

Smith, M. L., Bertram, A. K., and Martin, S. T.: Deliquescence, efflorescence, and phase miscibility of mixed particles of ammonium sulfate and isoprene-derived secondary organic material, Atmos. Chem. Phys., 12, 9613–9628, doi:10.5194/acp-12-9613-2012, 2012.

Surratt, J. D., Murphy, S. M., Kroll, J. H., Ng, N. L., Hildebrandt, L., Sorooshian, A., Szmigielski, R., Vermeylen, R., Maenhaut, W., Claeys, M., Flagan, R. C., and Seinfeld, J. H.: Chemical composition of secondary organic aerosol formed from the photooxidation of isoprene, J. Phys. Chem. A, 110, 9665–9690, doi:10.1021/jp061734m, 2006.

Surratt, J. D., Kroll, J. H., Kleindienst, T. E., Edney, E. O., Claeys, M., Sorooshian, A., Ng, N. L., Offenberg, J. H., Lewandowski, M., and Jaoui, M.: Evidence for organosulfates in secondary organic aerosol, Environ. Sci. Technol., 41, 517–527, 2007a.

Surratt, J. D., Lewandowski, M., Offenberg, J. H., Jaoui, M., Kleindienst, T. E., Edney, E. O., and Seinfeld, J. H.: Effect of acidity on secondary organic aerosol formation from isoprene, Environ. Sci. Technol., 41, 5363–5369, 2007b.

Surratt, J. D., Goìmez-Gonzaìlez, Y., Chan, A. W. H., Vermeylen, R., Shahgholi, M., Kleindienst, T. E., Edney, E. O., Offenberg, J. H., Lewandowski, M., and Jaoui, M.: Organosulfate formation in biogenic secondary organic aerosol, J. Phys. Chem. A, 112, 8345–8378, 2008.

Surratt, J. D., Chan, A. W. H., Eddingsaas, N. C., Chan, M. N., Loza, C. L., Kwan, A. J., Hersey, S. P., Flagan, R. C., Wennberg, P. O., and Seinfeld, J. H.: Reactive intermediates revealed in secondary organic aerosol formation from isoprene, P. Natl. Acad. Sci. USA, 107, 6640–6645, 2010.

Tanner, R. L., Olszyna, K. J., Edgerton, E. S., Knipping, E., and Shaw, S. L.: Searching for evidence of acid-catalyzed enhancement of secondary organic aerosol formation using ambient aerosol data, Atmos. Environ., 43, 3440–3444, 2009.

Wang, W., Kourtchev, I., Graham, B., Cafmeyer, J., Maenhaut, W., and Claeys, M.: Characterization of oxygenated derivatives of isoprene related to 2-methyltetrols in Amazonian aerosols using trimethylsilylation and gas chromatography/ion trap mass spectrometry, Rapid Commun. Mass Sp., 19, 1343–1351, 2005.

Yao, X., Rehbein, P. J. G., Lee, C. J., Evans, G. J., Corbin, J., and Jeong, C.-H.: A study on the extent of neutralization of sulphate aerosol through laboratory and field experiments using an ATOFMS and a GPIC, Atmos. Environ., 45, 6251–6256, doi:10.1016/j.atmosenv.2011.06.061, 2011.

Yasmeen, F., Szmigielski, R., Vermeylen, R., Gómez-González, Y., Surratt, J. D., Chan, A. W. H., Seinfeld, J. H., Maenhaut, W., and Claeys, M.: Mass spectrometric characterization of isomeric terpenoic acids from the oxidation of α-pinene, β-pinene, d-limonene, and Δ3-carene in fine forest aerosol, J. Mass Spectrom., 46, 425–442, doi:10.1002/jms.1911, 2011.

Zhang, H., Surratt, J. D., Lin, Y. H., Bapat, J., and Kamens, R. M.: Effect of relative humidity on SOA formation from isoprene/NO photooxidation: enhancement of 2-methylglyceric acid and its corresponding oligoesters under dry conditions, Atmos. Chem. Phys., 11, 6411–6424, doi:10.5194/acp-11-6411-2011, 2011.

Zhang, Z., Lin, Y.-H., Zhang, H., Surratt, J. D., Ball, L. M., and Gold, A.: Technical Note: Synthesis of isoprene atmospheric oxidation products: isomeric epoxydiols and the rearrangement products cis- and trans-3-methyl-3,4-dihydroxytetrahydrofuran, Atmos. Chem. Phys., 12, 8529–8535, doi:10.5194/acp-12-8529-2012, 2012.